THE JOURNAL OF PHYSICAL CHEMISTRY B

Article

pubs.acs.org/JPCB

Initial Events in the Degradation of Hyaluronan Catalyzed by Hyaluronate Lyase from *Spectrococcus pneumoniae*: QM/MM Simulation

Min Zheng,[†] Hongling Zhang,[‡] and Dingguo Xu*[,†]

[†]MOE Key Laboratory of Green Chemistry, College of Chemistry, Sichuan University, Chengdu, Sichuan, 610064 P. R China

[‡]College of Mathematics, Southwest Jiaotong University, Chengdu, Sichuan, 610031 P. R. China

Supporting Information

ABSTRACT: Hyaluronate lyase from *Spectrococcus pneumonia* can degrade hyaluronic acid, which is one of the major components in the extracellular matrix. The major functions of hyaluronan are to regulate water balance and osmotic pressure and act as an ion-exchange resin. In this work, we focus on the prerequisite issue of the enzymatic reaction, i.e., the initial reactive conformer. Based on the quantum mechanical and molecular mechanical molecular dynamic simulations and free energy profiles, a near attack conformer was obtained for the degradation of hyaluronan catalyzed by the hyaluronate lyase. Along with the substrate binding, the phenylhydroxyl hydrogen atom of Tyr408 will transfer to nearby His399 via a near barrierless transition state, which results in a negatively charged Tyr408 and positively charged His399. The Tyr408, rather than the previously proposed His399, was suggested to act as the general base for the subsequent β-elimination reaction. The His399 was suggested to have the function of neutralizing the C5-carboxyl group.

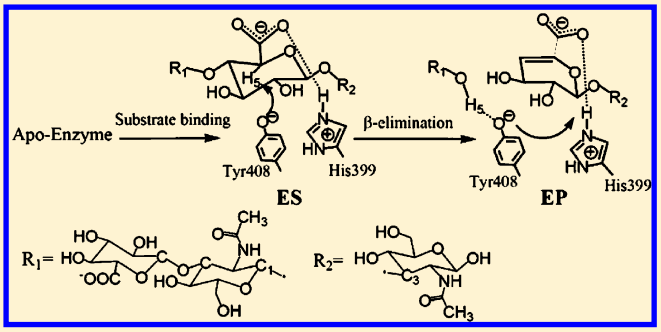

1. INTRODUCTION

The degradation of carbohydrates plays some crucial roles in many aspects including biomass conversion and human health problems. Two major types of enzymes, glycoside hydrolases (GHs)[1] and polysaccharide lyases (PLs),[2,3] have been identified for the degradation of glycosidic linkage but with different mechanisms. For GHs,[1] the hydrolytic mechanism to depolymerize the polysaccharides requires a water molecule in the active site, with either retention or inversion of the configuration at the C-1 anomeric carbon center.[4] The hydrolysis product usually contains a saturated hexaose ring on the nonreducing side. PLs, on the other hand, can cleave the uronic acid-containing polysaccharides via a β-elimination mechanism to generate an unsaturated hexenuronic acid residue. Currently, PLs are classified into 22 subfamilies according to the amino acid sequences, which is implemented in the CAZy (carbohydrate-active enzymes) database (http://www.cazy.org).[5]

For the nonhydrolytic cleavage of the glycosidic bond by lyases, the catalytic mechanisms have been discussed extensively.[2,3,6−8] A unified proton abstraction and donation (PAD) reactive process was proposed by Gacesa in 1987.[9] The reaction is involved with the neutralization of the substrate C5 carboxyl functionality, proton abstraction at C5, and syn or anti elimination of the 4-*O*-glycosidic bond to form a C4−C5 double bond. The general mechanisms are summarized in Scheme 1. One of key functions of the active site is suggested to

Scheme 1. General Mechanisms (syn and anti Elimination) for the Degradation of Uronic Acid Containing Polysaccharides Catalyzed by PLs[a]

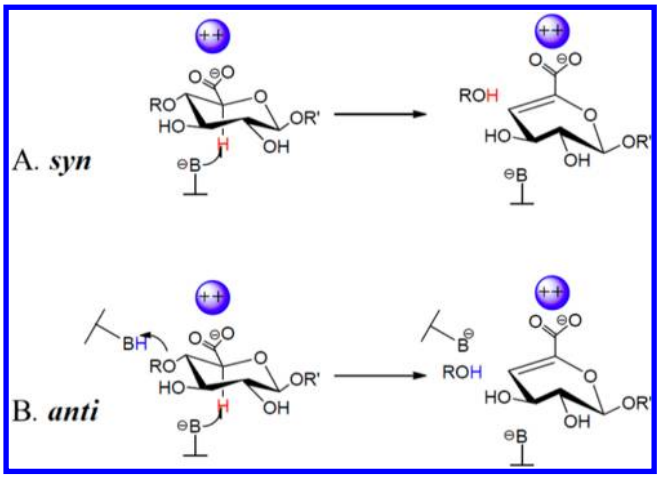

[a]The blue ball represents the neutralization groups, either metal ions or positively charged residues.

Received: July 8, 2012
Revised: August 20, 2012
Published: August 23, 2012

dx.doi.org/10.1021/jp306754a | *J. Phys. Chem. B* 2012, 116, 11166−11172

neutralize the C5 carboxyl group. Metal ion like Ca^{2+} is often found in the right position in some cases, e.g., pectate lyases.[2] In other cases, Asn or His residue is used to mediate the negative charge on the C5 carboxyl group, e.g., chondroitin AC lyase[10,11] from *Arthrobacter aurescens* and hyaluronate lyase from *Spectrococcus pneumoniae*.[12] It is basically a general base and general acid catalytic mechanism. The identities of general base and general acid are thus essential to understand the corresponding catalytic reaction. In this work, we will focus on the *S. pneumoniae* hyaluronate lyase (*SpnHL*).

SpnHL belongs to PL subfamily 8, which has an overall $\alpha/\alpha + \beta$ architecture. Major function of the *SpnHL* is to degrade hyaluronic acid (HA),[13−15] which is one of the major components of the extracellular matrix. The HA is a long polysaccharide, which is composed of repeating disaccharide unit linked together via β-1, 3-glycosidic bond. Each disaccharide unit consists of D-glucuronic acid (GlcUA) and *N*-acetyl-D-glucosomine (GlcNAc). HA can regulate water balance, osmotic pressure and act as an ion-exchange resin. The degradation mechanism is critical in many physiological processes, and the inhibitors studies to bacterial hyaluronidase are also important to pharmaceutical development.[16−19] In 2002, a high resolution structure of the *SpnHL* with hyaluronan tetrasaccharide substrate bound in the active site was reported, in which the key residue of Y408 was mutated to Phe residue.[12] The hyaluronan saccharide degradation mechanism of this enzyme is still under debate, especially in the identity of the general base. The possible catalytic mechanism suggested by Jedrzejas and co-workers[12,20−23] has following several major steps: (a) neutralization of C5-carboxyl group by N349 after the substrate bound in the binding cleft, (b) proton abstraction by H399, and followed by the formation of unsaturated bond between C4 and C5 atoms, (c) the cleavage of glycosidic bond facilitated by the proton donation from Y408.

However, this mechanism proposal was questioned by several groups[11,24] based on some facts related with this enzyme. First of all, the position of the imidazole group of H399 is as far as 3.66 Å away from the C5 atom, which makes the proton abstraction process difficult. Second, mutagenesis studies by Jedrejas et al. also indicate that Y408A completely deactivates the *SpnHL*,[12] while H399A still has some significant activity. Such observations could highlight the importance of the Y408 in the *SpnHL* catalyzed degradation of polysaccharide. It was then argued that the active site tyrosine residue (Y408) serves as the general base/general acid, while the functional role of the histidine residue (H399) is thought to help the substrate binding and neutralize the C5 carboxyl functionality. To better understand the mechanisms, numerous crystallographic structures for other members in the PL subfamily 8 have been reported, e.g, *Arthrobacter aurescens* Chondroitinase AC lyase,[11] *Bacillus sp.* Xanthan lyase.[24] According to the reported structures, the residues, which are important to the catalytic reaction including N349, H399, Y408 and R462 of *SpnHL*, are conserved in all of these enzymes. It is thus expected of similar catalytic mechanisms of enzymes in this subfamily. Indeed, if we carefully check the backbone of three polysaccharides, chondroitin AC, xathan, and hyaluronan, we can easily find a conserved GlcUA residue existing at the reducing end. For both chondroitin AC lyase and Xanthan lyase, the active site tyrosine residue was postulated to act as the general base to accept the C5 proton. If so, it should be deprotonated when the substrate molecule is bound in the active site. The issues would be addressed are where the proton goes and what the substrate binding pattern is for the native *SpnHL*. To correctly understand these questions, it is thus highly desirable to perform extensive theoretical simulations at the microscopic level. First of all, we aim to understand the substrate binding pattern using the combined quantum mechanical and molecular mechanical approach (QM/MM),[25] and then we will clarify the identity of the general base.

2. COMPUTATIONAL DETAILS

Due to unconquerable computational costs of the first principle methods on the systems like enzymes, a hybrid QM/MM approach has been extensively applied to address various functions of enzymes.[25] In QM/MM treatment, the whole system is divided into two parts, QM and MM regions. The smaller part (QM region) involving in bond-breaking and bond-forming processes is treated using high level quantum mechanical method. The rest of the system (MM region) including solvent molecules and protein atoms is described using a classical force field. The QM/MM method thus combines the accuracy of the QM method and the efficiency of the force field method.

To describe the QM region efficiently, the self-consistent charge-density functional tight binding (SCC-DFTB) method[26] was employed in this work, which has been implemented into the CHARMM package.[27] It has been widely tested for various enzyme systems,[27−31] including some glycosidases.[32,33] The CHARMM22 all atom force field was used to describe those atoms in the MM region.[34]

The initial model for the simulation was adopted from protein data bank (PDB code 1LXK[12] for a mutant *SpnHL* complexed with hyaluronan tetrasaccharide). As shown in Scheme 2, HA1 and HA2 are defined as the consecutive

Scheme 2. Atomic Definitions and Possible Interactions between Enzyme and the Tetrasaccharide[a]

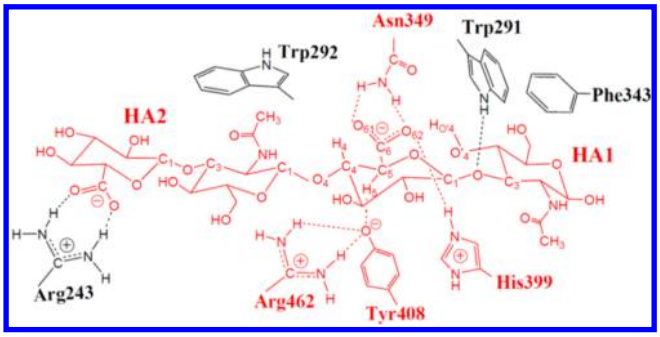

[a]The QM region is labelled using red. Dash lines represent possible hydrogen bond connections.

positions of hyaluronan disaccharide within the tetrasaccharide substrate numbered from the reducing toward the nonreducing end. The nomenclature of each atom for enzyme is adopted from the CHARMM definition. Hydrogen atoms were added to the heavy atoms using the HBUILD module. All of the polar residues are assigned to their correct protonation states judged by the environmental hydrogen bond network. The total system was first solvated in a pre-equilibrated TIP3P[35] water sphere of 25 Å radius centered at the C5 (HA1) atom. This process was repeated several times with rotated water spheres to ensure uniform solvation. The solvent was relaxed by 30 ps molecular dynamics (MD) with all protein and substrate atoms fixed. Stochastic boundary condition[36] was applied to reduce

the computational cost. In particular, those atoms outside a 25 Å radius away from the origin were removed. The link atom approach was applied to describe the covalent interface between QM and MM regions.[37] A total of 1.2 ns molecular dynamics (MD) simulations were then carried out to examine the stability or substrate binding information of the two systems. The system was, at first, slowly heated to 300 K over 30 ps, followed by 170 ps of equilibration. The subsequent 1 ns MD simulations were carried out, and the corresponding trajectory was saved for data analysis. The SHAKE algorithm[38] is applied to constrain the covalent bond involving hydrogen atoms. The integration time step is 1 fs. A group-based switching scheme was used for nonbonded interactions.[39]

3. RESULTS AND DISCUSSION

The accuracy of SCC-DFTB in the geometrical optimization has been extensively discussed. It was found that the SCC-DFTB optimized geometries could even compare well with those obtained at the B3LYP/6-31++G(d,p) level of theory.[40] For the particular system in this work, we have fully optimized the HA molecule at the B3LYP/6-31G(d,p) level of theory and compared it in Figure 1 with that obtained from the SCC-

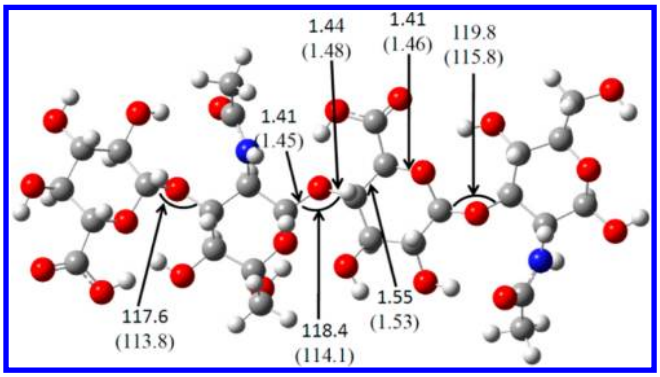

Figure 1. Comparison of selected geometries between B3LYP/6-31G(d,p) and SCC-DFTB (parentheses) optimized hyaluronan acid molecule. Units for distances are given in angstrom and degree for angles.

DFTB optimization with the convergence criterion that the rms gradient is less than 0.01 kcal/(mol Å^2). The geometrical properties from SCC-DFTB optimization are given in the parentheses. Clearly, the typical geometry differences between the SCC-DFTB and B3LYP results are less than 0.1 Å for bond distances, and 5° for glycosidic bond angles. Such small differences indicate that the SCC-DFTB method is reliable for describing geometries for relevant molecule. The density functional theory (DFT) calculations were performed using Gaussian 03 suite of program.[41]

To discuss the detailed catalytic process that occurrs in the enzyme active site, a reasonable enzyme−substrate (ES) complex structure is always in the core position. As we know, it is not that easy to get the direct complex structure with both native enzyme and the substrate molecule in an experimental way, as well as the *SpnHL*. The MD simulation, on the other hand, represents a possible way to predict a reasonable ES structure theoretically. Before we go further, it would be necessary to examine the stability of the apo *SpnHL* to examine the performance of the hybrid SCC-DFTB/CHARMM method. The initial structure for the apo enzyme is obtained from the protein data bank (PDB code 1EGU[21]) The setup protocol for the MD simulation is essentially the same as the one we did for the ES complex, but the side chain groups of H399 and Y408 are assigned to their neutral forms. The QM region consists of side chain atoms of N349, H399, Y408 and R462. The whole system is maintained very well throughout the simulation, evidenced by the root-mean-square deviation (rmsd) of 0.86 ± 0.07 Å for the backbone atoms compared to the crystal structure as shown in Figure 2. The topological

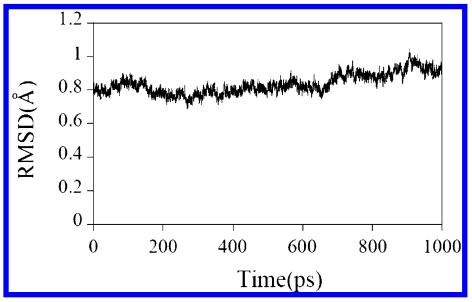

Figure 2. Root mean square deviation (rmsd) for the backbone atoms of the apo enzyme.

structure of the enzyme indicates that the overall protein is built from two distinct domains: a helical α-domain and a β-sheet β-domain. One of the snapshots extracted from the MD trajectory is given in Figure 3A, and an overlay representation

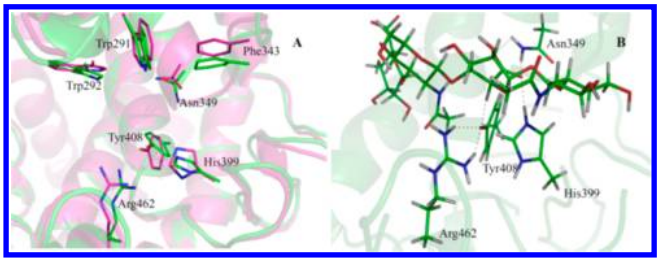

Figure 3. (A) Overlay representation between snapshot (carbon in green) extracted from the QM/MM MD trajectory and X-ray structure (carbon in purple) for apo *SpnHL*. (B) Snapshot of *SpnHL*-tetrasaccharide complex obtained from the QM/MM MD trajectory.

with the X-ray structure is also included to check the viability of combined SCC-DFTB/CHARMM method. The simulated overall structure has a good overlap with the X-ray structure. Some selected statistical averaged geometrical properties were listed in Table 1. Particularly, a stable hydrogen bond is found between H399 and Y408, with 1.78 ± 0.11 Å for the distance of HH(Y408)···NE2(H399). The corresponding distance of OH(Y408)···NE2(H399) is 2.74 ± 0.10 Å, which can be

Table 1. Selected Statistical Averaged Geometric Parameters for the apo SpnHL Obtained using the SCC-DFTB/CHARMM MD Simulation

distances (Å)	QM/MM MD	X-ray[21]
OH(Y408)···HH11(R462)	3.27 ± 0.76	
OH(Y408)···NH1(R462)	3.60 ± 0.64	3.53
OH(Y408)···HH21(R462)	2.51 ± 0.50	
OH(Y408)···NH2(R462)	2.93 ± 0.29	4.02
HH(Y408)···NH2(H399)	1.78 ± 0.11	
OH(Y408)···NE2(H399)	2.74 ± 0.10	3.19
HH(Y408)···OH(Y408)	0.98	

dx.doi.org/10.1021/jp306754a | J. Phys. Chem. B 2012, 116, 11166−11172

comparable with the experimental value of 3.19 Å. It should be noted that a significant difference could be found for the distance of OH(Y408) and NH2(R462) between the simulation and X-ray structures. Such a difference could be attributed to the different temperatures used in the MD simulation and the crystallization. Nevertheless, without the substrate, no stable hydrogen bond can be formed between Y408 and R462 either in the apo enzyme or in our MD simulation.

For the enzyme−substrate (ES) complex, we simply replaced F408 with Y408 to restore its native structure. The QM region consists of a whole substrate molecule and side chain atoms of N349, H399, Y408, and R462, resulting in a total of 152 atoms. To avoid artificial effect, we first built a model which follows the proposal by Jedrzejas and co-workers;[12] that is, the side chain groups of Y408 and H399 are in their neutral form (neutral model). The HH atom of Y408 was not included in the SHAKE list to check its flexibility. Interestingly, this hydrogen atom was found to spontaneously transfer to the NE2 atom of H399 within a very short time (about 15 ps), even in the heating stage. Such behavior generates a negatively charged tyrosine residue (Y408) and a positively charged histidine residue (H399). This proton could not transfer back to Y408 to recover the original model in the additional 185 ps simulation as shown in Figure 4. After the proton transfer, the H399 points

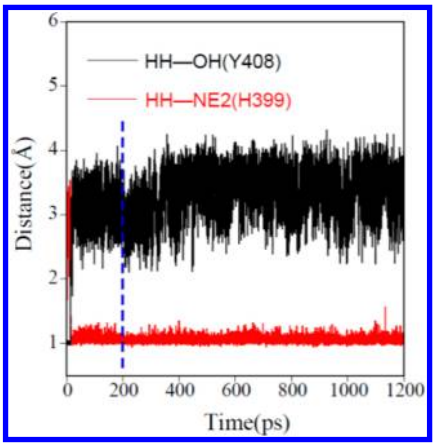

Figure 4. Distances of HH(Y408)···OH(Y408) and HH(Y408)···OH-(H399) along the time trajectory for the enzyme−substrate complex.

to the C5-caboxylate group of the GlcUA residue instead of the hydrogen bond with Y408. Such an unambiguous protonation state and stable hydrogen bond interaction might indicate that H399 cannot serve as the general base in the subsequent catalytic reaction. We thus take the ionized model (shown in Scheme 2) in the following simulations, in which the Y408 is assigned as the ionized state and the H399 bears a positive charge. The hydrogen atom is still labeled as HH for convenience. This structure is then consistent with suggestions from Maruyama et al., in which a nearby tyrosine should act as the general base before the β-elimination.[24] Mutagenesis studies have demonstrated that Y408 is critical in the catalytic cycle since the Y408F mutation completely deactivates the enzyme.

The complex system was then subjected to an additional 1 ns QM/MM MD simulation to obtain the substrate binding information. One snapshot from the MD trajectory was depicted in Figure 3B, and some selected statistical averaged geometrical parameters were summarized in Table 2. The

Table 2. Selected Statistical Averaged Geometric Parameters for the SpnHL-Tetrasaccharide Complex Obtained Using SCC-DFTB/CHARMM MD Simulation

distances (Å)	QM/MM MD	X-ray[12]
OH(Y408)···HH11(R462)	1.75 ± 0.11	
OH(Y408)···HH21(R462)	1.97 ± 0.19	
HH(Y408/H399)···NE2(H399)	1.06 ± 0.04	
HH(Y408/H399)···OH(Y408)	3.34 ± 0.36	
O4(HA1)···HH21(R462)	2.34 ± 0.20	3.02[a]
O4(HA1)···OH(Y408)	3.36 ± 0.23	
C5(HA1)···NE2(H399)	3.59 ± 0.18	3.66
H5(HA1)···OH(Y408)	1.94 ± 0.12	
O61(HA1)···HH21(N349)	2.04 ± 0.29	3.56[a]
O62(HA1)···HH21(N349)	2.48 ± 0.43	
O62(HA1)···OD1(N349)	3.67 ± 0.24	3.12
O62(HA1)···HH(Y408/H399)	1.72 ± 0.15	
O62(HA1)···NE2(H399)	2.72 ± 0.11	3.33[a]
HO′4(HA1)···O62(HA1)	1.87 ± 0.14	3.09[b]
O3(HA1)··· HE1(W291)	2.39 ± 0.32	2.87[a]
O61(HA2)···HH11(R243)	1.78 ± 0.25	
O62(HA2)···HH21(R243)	1.91 ± 0.31	

[a]Distance of O−N. [b]Distance of O−O.

polysaccharide molecule was found to stay in the binding cleft quite tightly, which is stabilized by the significant hydrogen bond network formed by the enzyme active site residues such as R243, W291, N349, and H399. The side chain group of N349 points directly to the C5-carboxylate group of the HA1 unit with the distance of 2.04 ± 0.29 Å for O61(HA1)···HH21-(N349). However, it looks like the previously proposed function of the charge neutralization for this residue is not so strong. The GlcUA residue of HA2 is stabilized by R243 with a hydrogen bond formed between the C5-carboxylate group and the guanidinium group, evidenced by the distances of 1.78 ± 0.25 and 1.91 ± 0.31 Å for O61(HA2)···HH11(R243) and O62(HA2)···HH21(R243), respectively. Instead of hydrophobic interaction with the substrate molecule, the hydrogen bond formed between W291 and the glycosidic oxygen atom (O3) of the HA1 unit, 2.39 ± 0.32 Å for O3···HE1(W291), can provide additional stabilization for the substrate sugar. Additionally, it is common that the hydrophobic stacking interaction between hydrophobic residues and sugar rings could help the polysaccharide molecules binding in the carbohydrate active enzymes. In the current system, such behaviors can also be observed, e.g., the indole group of W292 is almost in parallel position to the GlcNAc unit of HA2 residue, and the GlcNAc unit of HA1 residue is stabilized by the aromatic ring of F343. During the simulation, it was found that the phenyl hydroxide ion of Y408 is reoriented by R462. The distances of OH(Y408)···HH11(R462) and OH(Y408)···HH21(R462) are 1.75 ± 0.11 and 1.97 ± 0.19 Å, respectively. This hydrogen bond network could make the Y408 stay in a suitable position ready for the abstraction of the C5 proton. Indeed, a shorter distance of 1.94 ± 0.12 Å between the OH atom of Y408 and the H5 atom of GlcUA indicates the possibility of the general base for the Y408. Meanwhile, the distance between the glycosidic oxygen atom (O4) and hydroxide oxygen atom (OH) of Y408 is found to be 3.36 ± 0.23 Å, suggesting that Y408 abstracts the proton on the C5 atom of GlcUA residue and is the general acid in the following cleavage of the glycosidic bond. Obviously, it is highly desirable to perform further calculations to confirm these proposals, which is

dx.doi.org/10.1021/jp306754a | J. Phys. Chem. B 2012, 116, 11166−11172

underway in our lab. No direct interaction can be found between Y408 and H399 throughout the simulation. Instead, H399 forms a strong hydrogen bond with the C5-carboxylate group of the GlcUA unit, with the distance of 1.72 ± 0.15 Å between HH and O62. This is in good agreement with the experimental value of 3.33 Å for the distance between NE2(H399) and O62 atoms.[12] Such an observation might suggest that the major function of H399 can help the binding of the substrate molecule and neutralization of the carboxylate group, since it is the only residue that bears the positive charge close to the C5-carboxyl group. As no hydrogen bond between the H5 atom of GlcUA and H399 is formed during the simulation, it is unlikely for H399 to act as the general base for the β-elimination. In addition, it is not unique that the tyrosine residue acts as the base catalyst in the polysaccharide lyases. Similar performance for the tyrosine residue could be observed in the catalyzed conversion of L-asparagine to L-aspartic acid by the bacterial asparaginases.[42] The Y25 takes the ionized form first by transferring the proton to nearby E283, and then serve as the base to activate the Thr12 to complete the reaction.

Our MD simulations suggested that the HH atom of Y408 can automatically transfer to H399 due to binding of the substrate molecule. It is thus necessary to examine if such proton transfer can be induced by the binding of the substrate molecule. To do this, we further calculated potentials of mean force (PMF) on the proton transfer between H399 and Y408 with and without the substrate in the active site, respectively. The reaction coordinate for the proton transfer is then defined as $d = d_{HH(Y408)\cdots OH(Y408)} - d_{HH(Y408)\cdots NE2(H399)}$ for both apo and complex structure. We first calculated the minimum energy path (MEP) along the putative reaction coordinate using adiabatic mapping approach. The obtained structures were then used for the following MD simulations. Umbrella sampling[43] with a harmonic constraint of around 50 kcal/(mol Å^2) was applied to enhance sampling. Totals of 25 and 18 windows were used for apo and complex structures, respectively. For each window, the first 40 ps for heating and equilibration and subsequent 60 ps simulation trajectory were saved for data analysis. The weighted histogram analysis method (WHAM)[44] was used to obtain the PMF. The activation energy barrier heights of proton transfer for both apo and complex structures are listed in Table 3. Figure 5A gives the corresponding free energy profile for this proton transferring from Y408 to H399 in the apo enzyme. As we can see, this neutral model has to overcome about 3.0 kcal/mol to reach the positive H399 (ionized model), which has a relatively shallow potential well of 0.24 kcal/mol. It also indicates that the neutral model is more stable than the ionized structure in the case of the apo enzyme. In other words, we might suggest the following possibility; that is, once the degradation reaction is completed and the reducing species is released from the active site, the easy proton transfer from H399 to Y408 could restore the native catalyst to complete the whole catalytic cycle. On the other hand, when the substrate molecule is bound in the active site, the proton cannot spontaneously transfer back to Y408 from H399 as shown in Figure 5B. This can be understandable since there is no hydrogen bond formed between Y408 and H399 as shown by our QM/MM MD simulations. Meanwhile, if we take a look at the process from neutral model to ionized model, the hydroxyl hydrogen atom of Y408 can transfer to H399 via a nearly barrierless transition state (ΔG = 0.22 kcal/mol) according to Table 3 and Figure 5B, which is consistent with our MD simulation. It is unlikely that he minimum around d = 0.0 Å is the formation of an ionized tyrosine residue, because the proton transfer does not complete yet. It is probably due to some local conformational minimum in the active site. Overall, combining the free energy profiles for apo and complex enzyme structures, it could be postulated that the proton transfer is induced by the binding of the substrate molecule.

Table 3. Activation Energy Barriers for the Proton Transfer Reactions in apo and Complex Structures

model	ΔG (kcal/mol)
apo enzyme	3.0
complex	0.22

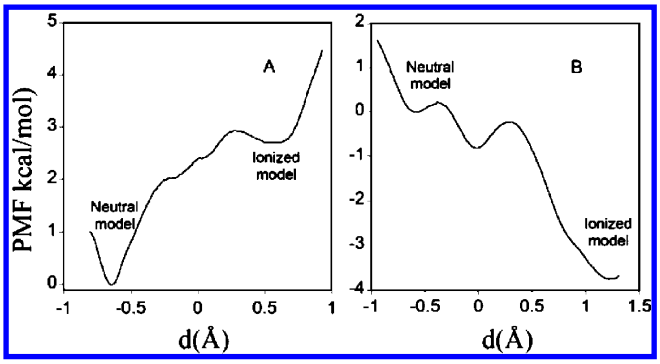

Figure 5. Potentials of mean force for the proton transfer between H399 and Y408. Panel A is for proton transfer occurred in the apo enzyme, and panel B is for the complex structure.

For enzymatic reactions, a preorganization process will undergo for both substrate molecule and enzyme with the binding of substrate into the active site. This could result in the so-called near attack conformation, which is introduced by Bruice et al.[45,46] for understanding the origin of enzyme catalysis. Such phenomena are prevalent in the enzymatic reactions, e.g., for the Class3 aldehyde dehydrogenase,[47] QM/MM simulations suggested that the C243 is initially in its neutral form, while the substrate binding could induce the deprotonation of C243 to form a thiolate group that is ready for subsequent nucleophilic attack at the substrate molecule. Besides that, the substrate itself could also adjust its conformation to facilitate the access by catalyst, e.g., the binding of cellotetraose into the cellulase 5A from *Acidothermus cellulolyticus* leads to the bending of the sugar chain to fit the binding cleft.[32]

The classical MD simulations of apo *SpnHL* and *SpnHL*-polysaccharides complex have been performed to check the domain flexibility of the binding cleft by Rigden et al.[48] This could be used to investigate the processive mechanism of *SpnHL*. Unfortunately, it does not provide direct geometric information for the catalytic mechanism. The QM/MM MD simulations reported in this work indicate that the Y408 is in an ionized state, and H399 is positively charged in the presence of the substrate molecule. More importantly, a quite strong hydrogen bond is formed between the positively charged H399 residue and the C5-carboxylate group of the GlcUA residue. Such geometric properties could suggest that the initial charge neutralization of C5-carboxylate group will be provided by H399 residue with no doubt. According to the position of Y408, a possible syn-elimination mechanism is then summarized in Scheme 3, in which the Y408 is the general base for the first step of the formation of a double bond between C4 and C5

Scheme 3. Proposed Catalytic Mechanism in the Degradation of Hyaluronan Tetrasaccharide molecule catalyzed by *SpnHL*

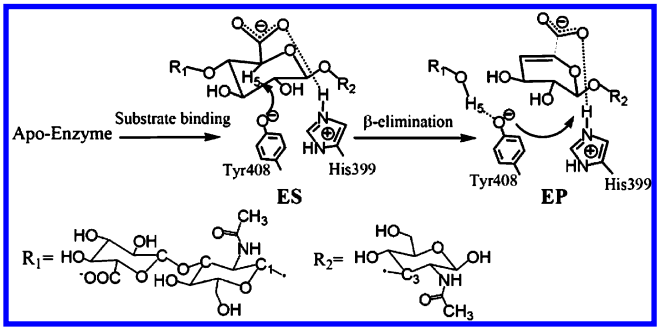

atoms and the general acid for the second step to facilitate the cleavage of glycosidic bond. Future simulations will be devoted to verify this proposal. Notably, our results are consistent with the mechanisms proposed for the members in the same subfamily, including chondoitin AC lyase[11] and xanthan lyase.[24] Finally, our simulations also provide evidence of the importance of the enzyme reorganization process with the binding of the substrate molecule. Such kind of reorganization could result in a near attacking conformer (NAC),[45] for which the Y408 is in its correct protonation state and suitable position, for the subsequent catalytic reaction.

4. CONCLUSION

In this work, we investigated the substrate binding pattern for the *SpnHL* complexed with a hyaluronan tetrasaccharide molecule. The present QM/MM MD simulations demonstrate that there is nearly no energy barrier to form a NAC for the enzyme catalyzed degradation of the hyaluronan. The active site tyrosine (Y408) was proposed to be in its ionized state with the binding of substrate molecule. Meanwhile, the nearby histidine residue (H399) is then protonated to neutralize the C5-carboxyl group. Based on our simulation results, we further proposed a *syn*-elimination mechanism for the degradation of the hyaluronan tetrasaccharide molecule, in which Y408 is thought to be the general base/acid catalyst. It can be seen that a unified mechanism will then be shared for members in the PL8 subfamily. Therefore, further simulations will focus on the confirmation of the current mechanism proposal for Y408 and H399 and determine that the overall catalytic reaction process is via a stepwise or a concerted pathway.

■ ASSOCIATED CONTENT

Ⓢ Supporting Information

Full citations for refs 28, 34, and 41. Figures of two transition states for the proton transfer in the apo and complex structures. This material is available free of charge via the Internet at http://pubs.acs.org.

■ AUTHOR INFORMATION

Corresponding Author

*E-mail: dgxu@scu.edu.cn.

Notes

The authors declare no competing financial interest.

■ ACKNOWLEDGMENTS

This work was funded by National Science Foundation of China (Nos. 21073125 and 31170675) and by the Program for New Century Excellent Talents in University (No. NCET-10-0606) to D.X. This work was also supported by the Fundamental Research Funds for the Central Universities (No. A0920502051202-111) to H.Z. Parts of the results described in this paper are obtained on the Deepcomp7000 of Supercomputing Center, Computer Network Information Center of Chinese Academy of Sciences.

■ REFERENCES

(1) Henrissat, B.; Davies, G. *Curr. Opin. Struct. Biol.* **1997**, *7*, 637−644.
(2) Garron, M.; Cygler, M. *Glycobiology* **2010**, *20*, 1547−1573.
(3) Lombard, V.; Bernard, T.; Rancurel, C.; Brumer, H.; Coutinho, P. M.; Henrissat, B. *Biochem. J.* **2010**, *432*, 437−444.
(4) Koshland, D. E. J. *Biol. Rev.* **1953**, *28*, 416−436.
(5) Cantarel, B. L.; Coutinho, P. M.; Rancurel, C.; Bernard, T.; Lombard, V.; Henrissat, B. *Nucleic Acids Res.* **2009**, *37*, D233−D238.
(6) Gasesa, P. *FEBS Lett.* **1987**, *212*, 199−202.
(7) Yip, V. L.; Withers, S. G. *Curr. Opin. Chem. Biol.* **2006**, *10*, 147−155.
(8) Yip, V. Y.; Withers, S. G. *Org. Biomol. Chem.* **2004**, *2*, 2707−2713.
(9) Gacesa, P. *FEBS Lett.* **1987**, *212*, 199−202.
(10) Rye, C. S.; Withers, S. G. *J. Am. Chem. Soc.* **2002**, *129*, 9756−9767.
(11) Lunin, V. V.; Li, Y.; Linhardt, R. J.; Miyazono, H.; Kyogashima, M.; Kaneko, T.; Bell, A. W.; Cygler, M. *J. Mol. Biol.* **2004**, *337*, 367−386.
(12) Jedrzejas, M. J.; Mello, L. V.; de Groot, B. L.; Li, S. *J. Biol. Chem.* **2002**, *277*, 28287−28297.
(13) Laurent, T. C.; Fraser, J. R. E. *FASEB J.* **1992**, *6*, 2397−2404.
(14) Lin, B.; Hollingshead, S. K.; Coligan, J. E.; Egan, M. L.; Baker, J. R.; Pritchard, D. G. *J. Biol. Chem.* **1994**, *269*, 30113−30116.
(15) Pritchard, D. G.; Lin, B.; Willingham, T. R.; Baker, J. R. *Ar. Biochem. Biophys.* **1994**, *315*, 431−437.
(16) Stern, R. *Eur. J. Cell Biol.* **2004**, *83*, 317−325.
(17) Botzki, A.; Rigden, D. J.; Braun, S.; Nukui, M.; Salmen, S.; Hoechstetter, J.; Bernhardt, G.; Dove, S.; Jedrzejas, M. J.; Buschauer, A. *J. Biol. Chem.* **2004**, *279*, 45990−45997.
(18) Yadav, G.; Prasad, R. L. A.; Jha, B. K.; Rai, V.; Bhakuni, V.; Datta, K. *J. Biol. Chem.* **2009**, *284*, 3897−3905.
(19) Hynes, W. L.; Walton, S. L. *FEMS Microbiol. Lett.* **2000**, *183*, 201−207.
(20) Ponnuraj, K.; Jedrzejas, M. J. *J. Mol. Biol.* **2000**, *299*, 885−895.
(21) Li, S.; Kelly, S. J.; Lamani, E.; Ferraroni, M.; Jedrzejas, M. J. *EMBO J.* **2000**, *19*, 1228−1240.
(22) Stern, R.; Jedrzejas, M. J. *Chem. Rev.* **2006**, *106*, 818−839.
(23) Stern, R.; Jedrzejas, M. J. *Chem. Rev.* **2008**, *108*, 5061−5085.
(24) Maruyama, Y.; Hashimoto, W.; Mikami, B.; Murata, K. *J. Mol. Biol.* **2005**, *350*, 974−986.
(25) Warshel, A.; Levitt, M. *J. Mol. Biol.* **1976**, *103*, 227−249.
(26) Elstner, M.; Porezag, D.; Jungnickel, G.; Elsner, J.; Haugk, M.; Frauenheim, T.; Suhai, S.; Seigert, G. *Phys. Rev.* **1998**, *B58*, 7260−7268.
(27) Cui, Q.; Elstner, M.; Kaxiras, E.; Frauenheim, T.; Karplus, M. *J. Phys. Chem. B* **2001**, *105*, 569−585.
(28) Riccardi, D.; Schaefer, P.; Yang, Y.; Yu, H.; Ghosh, N.; Prat-Resina, X.; Konig, P.; Li, G.; Xu, D.; Guo, H.; et al. *J. Phys. Chem. B* **2006**, *110*, 6458−6469.
(29) Otte, N.; Scholten, M.; Thiel, W. *J. Phys. Chem. A* **2007**, *111*, 5751−5755.
(30) Wu, S.; Xu, D.; Guo, H. *J. Am. Chem. Soc.* **2010**, *132*, 17986−17988.
(31) Xu, D.; Guo, H. *J. Am. Chem. Soc.* **2009**, *131*, 9780−9788.
(32) Liu, J.; Wang, X.; Xu, D. *J. Phys. Chem. B* **2010**, *114*, 1462−1470.
(33) Liu, J.; Jin, Y.; Xu, D. *J. Mol. Graph. Mod.* **2012**, *37*, 67−76.
(34) MacKerell, A. D., Jr.; Bashford, D.; Bellott, M.; Dunbrack, R. L., Jr.; Evanseck, J. D.; Field, M. J.; Fischer, S.; Gao, J.; Guo, H.; Ha, S.; M..; et al. *J. Phys. Chem.* **1998**, *B102*, 3586−3616.

(35) Jorgensen, W. L.; Chandrasekhar, J.; Madura, J. D.; Impey, R. W.; Klein, M. L. *J. Chem. Phys.* **1983**, *79*, 926−935.
(36) Brooks, C. L., III; Karplus, M. *J. Mol. Biol.* **1989**, *208*, 159−181.
(37) Field, M. J.; Bash, P. A.; Karplus, M. *J. Comput. Chem.* **1990**, *11*, 700−733.
(38) Ryckaert, J.-P.; Ciccotti, G.; Berendsen, H. J. C. *J. Comput. Phys.* **1977**, *23*, 327−341.
(39) Steinbach, P. J.; Brooks, B. R. *J. Comput. Chem.* **1994**, *15*, 667−683.
(40) Elstner, M.; Cui, Q.; Munih, P.; Kaxiras, E.; Frauenheim, T.; Karplus, M. *J. Comput. Chem.* **2003**, *24*, 565−581.
(41) Frisch, M. J.; et al. Gaussian 03, revision A.1; Gaussian, Inc.: Pittsburgh, PA, 2003.
(42) Sanches, M.; Krauchenco, S.; Polikarpov, I. *Curr. Chem. Biol.* **2007**, *1*, 75−86.
(43) Torrie, G. M.; Valleau, J. P. *J. Comput. Phys.* **1977**, *23*, 187−199.
(44) Kumar, S.; Bouzida, D.; Swendsen, R. H.; Kollman, P. A.; Rosenberg, J. M. *J. Comput. Chem.* **1992**, *13*, 1011−1021.
(45) Lightstone, F. C.; Bruice, T. C. *J. Am. Chem. Soc.* **1996**, *118*, 2595−2605.
(46) Bruice, T. C.; Lightstone, F. C. *Acc. Chem. Res.* **1999**, *32*, 127−136.
(47) Wymore, T.; Deerfield, D. W., II; Field, M. J.; Hempel, J.; Nicholas, H. B., Jr. *Chemico-Biol. Inter.* **2003**, *143*−*144*, 75−84.
(48) Rigden, D. J.; Littlejohn, J. E.; Joshi, H. V.; de Groot, B. L.; Jedrzejas, M. J. *J. Mol. Biol.* **2006**, *358*, 1165−1178.